The 2022 World Congress on
The 2022 Structures Congress (Structures22)
16-19, August, 2022, GECE, Seoul, Korea

Static stability of a submerged floating tunnel module in wet tow

*Ikjae Lee[1)], Chungkuk Jin[2)] and Moohyun Kim[3)]

[1), 3)] *Department of Ocean Engineering, Texas A&M University, College Station, TX, 77845, USA*
[2)] *Department of Ocean Engineering and Marine Sciences, Florida Institute of Technology, Melbourne, FL, 32901, USA*
[*] *ijlee@tamu.edu*

ABSTRACT

A case study for a submerged floating tunnel module (SFTM) in wet tow condition is carried out. Motivated by successful wet tow applications of spar platforms, several wet tow scenarios, in which a tunnel module horizontally afloat with half-diameter draft is towed by tugboats using towing lines, are studied. In order to investigate the static stability of the SFTM under wet-tow condition, numerical static offset tests are performed for different tow speeds and towline angles to obtain equivalent stiffness. The static offset tests include surge, sway, yaw and roll motions. The roll hydrostatic restoring moment of a horizontally floating circular cylinder with half-diameter draft is nearly zero when the geometric center coincides with the mass center, and thus it is essential to check roll stability with the given configuration of towing lines. Moreover, the effects of pre-tension resulting from different line arrangements and tow speeds are investigated. Numerical results are illustrated to evaluate the static stability of the present wet tow scenarios.

1. INTRODUCTION

Motivated by successful wet tow operations of spar platforms (Wang et al., 2003 and Sherman et al., 2019), similar horizontal wet tow scenarios for a SFTM using tugboats and towing lines, are considered. In the aforenoted papers, the seakeeping performance of the towed object is investigated. However, the present study more focused on the static stability problem of the SFTM in several wet tow conditions.

In this study, numerical static offset tests are performed for four modes of SFTM motions that include surge, sway, roll and yaw. They are done for different tow speeds and towline angles to obtain the respective equivalent stiffnesses of the system so that we may evaluate the static stability of the wet tow system for each case. There are several ways of obtaining equivalent stiffnesses either analytically or numerically (Amaral et al, 2022 and Kim et al., 2013). However, the previous studies are mostly restricted to

---

[1)] PhD Student
[2)] Assistant Professor
[3)] Professor

the stationary moored structures, and to the authors' best knowledge, little has been done for the towing problems.

A sequential procedure for the numerical static offset tests is suggested and performed for surge, sway, roll and yaw motions. Pre-tensions due to different tow speeds are investigated. Also, the roll hydrostatic restoring moment of a horizontally floating circular cylinder with half-diameter draft is nearly zero when the geometric center coincides with the mass center, equivalent metacentric heights for the coupled wet towing system are obtained.

In Section 2, static stability of the SFTM is discussed. In Section 3, numerical results are given, which is followed by Section 4 conclusions.

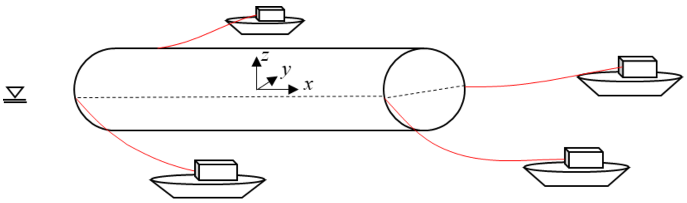

Fig. 1 A sketch for a wet tow scenario

2. STATIC STABILITY OF COUPLED SYSTEM

The static stability of the coupled system is investigated in this section. Intact stability for the roll motion is discussed, and a stepwise procedure for the static offset tests is suggested.

2.1. Intact stability

The transverse metacentric height ($\overline{GM_T}$) of the SFTM becomes zero unless the center of gravity is non-zero as

$$\overline{GM_T} = \frac{I_{yy}^{WP}}{\nabla} + z_B - z_G = -z_G \tag{1}$$

where ∇ is the displaced volume of the SFTM, I_{yy}^{WP} is the second moment of waterplane area with respect to *x*-axis, z_B and z_G are center of buoyancy and gravity, respectively. As shown above, the metacentric height reduces to a vertical coordinate of the center of gravity in negative sign due to a unique nature of the SFTM geometry. We will investigate later how much the towlines contribute to the roll stability in the form of equivalent metacentric height.

2.2. Static offset test in wet tow conditions

A sequential procedure for the offset tests is summarized in the flow chart in Fig. 2. We subdivide the offset test into several sub-steps, and at each sub-step, we impose incremental loads to get converged solutions. The same procedure is repeated for different motions, tow speeds and towline angles, ψ, at fairleads shown in Fig. 3. Four tugs are arranged in parallel, and they tow the SFTM with equally distributed towline tensions. The range of input parameters and wet tow conditions used for computation are tabulated in Table 1. Principal dimensions of the SFTM and towlines are given in Table 2.

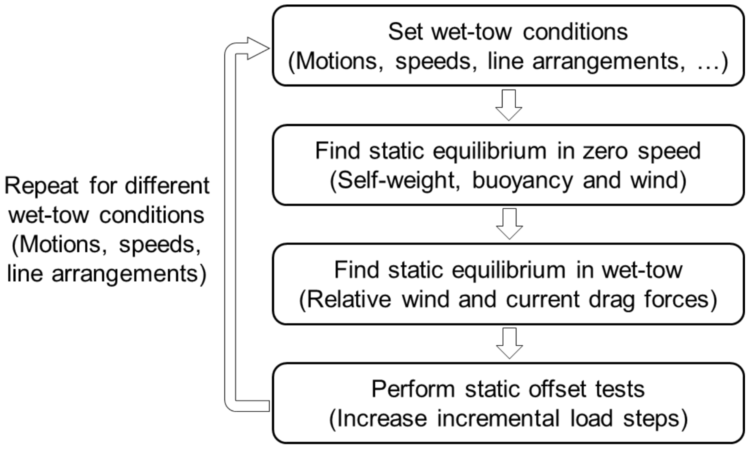

Fig. 2 Flow chart of static offset tests

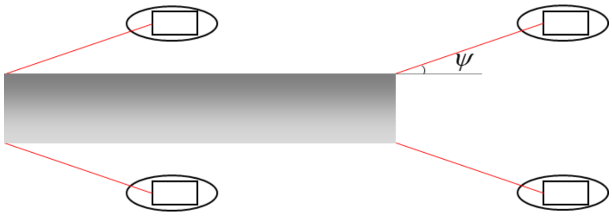

Fig. 3 A wet-tow configuration: birds-eye view

Table 1 Wet tow conditions

Motions	Surge, sway, roll and yaw
Tow speeds (m/s)	0, 1, 2, 3, 4
Wind speed (10m above MWL) (m/s)	6
Angles (ψ) at fairleads (degree)	35, 40, 45
Water depth (m)	80

Table 2 Principal dimensions of the SFTM and towlines

SFTM	Length (m)	160
	Diameter (m)	23
	Draft (m)	11.5
	Transverse metacentric height ($\overline{GM_T}$) (m)	0.1
	Drag coefficients in air (tangential / normal)	0.82 / 0.4
	Drag coefficients in water (tangential / normal)	0.82 / 0.4
Towlines	Density (kg/m^3)	1500
	Unstretched length (m)	60
	Axial stiffness (kN)	1.5×10^5
	Constraint at SFTM	Hinged

	Constraint at Tugboats	Clamped (fixed ψ)
	Drag coefficients in water (tangential / normal)	0.01 / 1.2

4. NUMERICAL RESULTS

A Total Lagrangian formulation of a curved beam finite element method (Dvorkin et al., 1988) for the towing lines and rigid body SFTM motions are fully coupled based on the method of Lagrange multipliers in the form of essential boundary conditions. In addition to aero- and hydrodynamic viscous drags, Munk moment is also considered. More details about the Munk moment can be found in Triantafyllou and Hover (2003). Since the Munk moment contains the added masses of zero-frequency, a reliable 3D panel code WAMIT is used (Lee, 1995). In addition, finite rotation effects for both the towlines and the SFTM are taken into consideration based on Rodrigues' rotation formula (Dvorkin et al., 1988).

Since the towlines are modeled by continuum-based 3D beam finite element model, iterative solutions of a very small bending stiffness do not converge well for some wet tow conditions. To avoid such a numerical barrier, towline diameter is increased up to 0.24m while maintaining axial stiffness of a steel wire rope employed by MARIN (Maritime Research Institute Netherlands) in OCIMF (2020) as given in Table 2.

First, pre-tensions are calculated for different tow speed and towline angles in Fig. 4, as they are determined by towing resistance. The pre-tensions are measured at positions close to the fairleads. Based on these static equilibriums, static offset tests are performed by imposing incremental load steps on the SFTM in Fig. 5.

4.1. Pre-tensions

It is observed from Fig. 4 that different towline angles can affect the pre-tensions although they are connected with one another based on hinged conditions. As pre-tensions in most cases positively affect the restoring of coupled systems, we restrict the range of offset tests to the cases of $\psi = 45^\circ$ that have slightly higher pre-tensions over the other two cases.

4.2. Offset test results

The offset test results are given in Fig. 5. Except for the roll motion, pre-tensions from different tow speeds play a significant role in the restoring of the coupled system. As discussed earlier, the intact stability of the roll motion is very small. In this regard, equivalent stiffnesses are represented in the form of equivalent $\overline{GM}_T$ that can be calculated by the equivalent stiffness with the weight force of the SFTM as given in Table 3. Recalling that the initial $\overline{GM}_T$ is 0.1 m that is a minimum value artificially given to avoid a numerically unstable system, additional restoring from the towlines is marginal, which is at most 0.07 m for 4 m/s tow speed. As mentioned earlier, however, the pressure loads acting normal to the outer surface of the body point toward the geometric center of the SFTM, and the geometric center is located very close to the center of rotation. Thus, moment arms for those from the aerodynamic and hydrodynamic pressures are extremely small. Considering that the tangential stresses acted upon the SFTM are also very small, even the small increase of the restoring from towlines might be able to resist the roll moment.

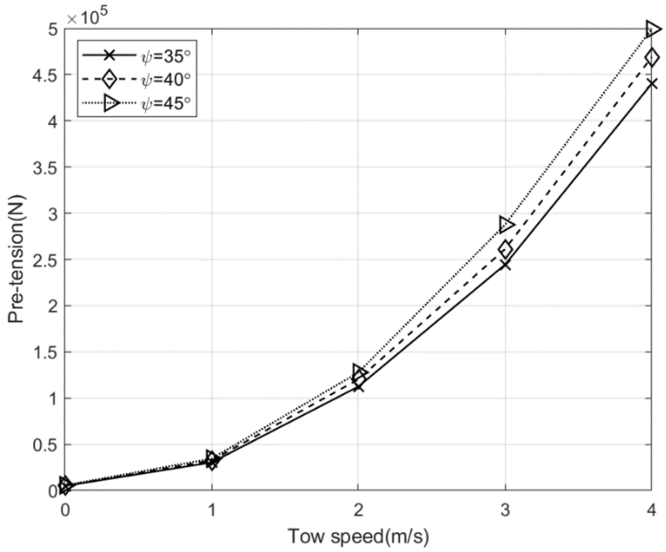

Fig. 4 Variation of pre-tensions for different angles and tow speeds

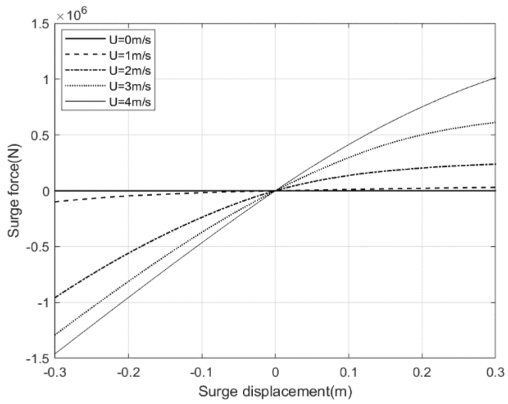

(a) Surge

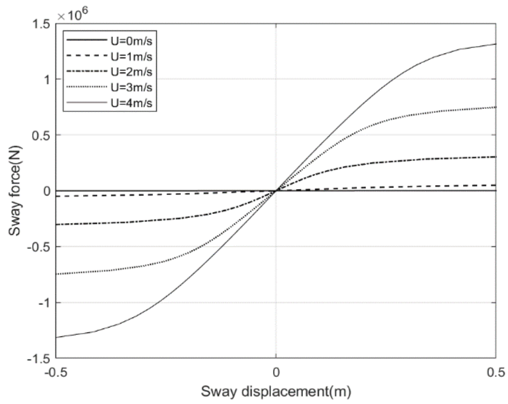

(b) Sway

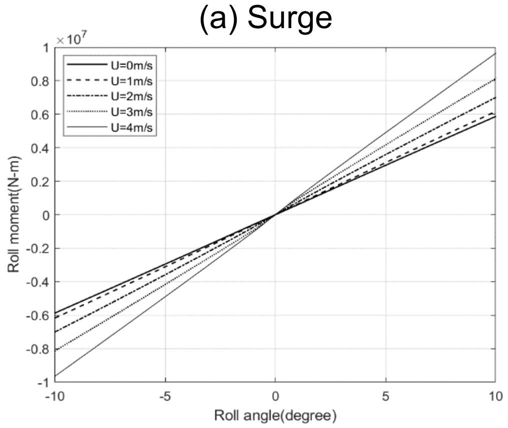

(c) Roll

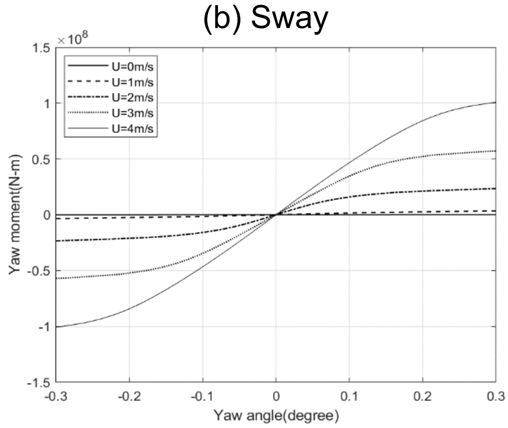

(d) Yaw

Fig. 5 Static offset test results

Table 3 Equivalent GM_T (transverse Metacentric height) for varying tow speeds

U(m/s)	0	1	2	3	4
Equiv. GM_T (m)	0.1014	0.1072	0.1257	0.1507	0.1733

5. CONCLUSIONS

A static stability analysis for the SFTM in wet tow condition has been performed. A sequential procedure for the static offset tests was suggested and performed. Pre-tensions for different tow speeds and towline angles are calculated, and then the static offset tests were performed for four different rigid body modes and different tow speeds. Due to the unique nature of the SFTM geometry, nearly zero roll stability was demonstrated through the intact stability formula, and equivalent stiffnesses were calculated in the form of equivalent $\overline{GM}_T$. The numerical results have shown that the towlines slightly increase the system's stability. However, even the small increase of the restoring from towlines might be able to resist the roll moment.

REFERENCES

Wang, J. J., Lu, R. and Lu, N. (2003). "Truss spar strength and fatigue analysis for wet tow." *Proceedings of the Thirteenth (2003) International Offshore and Polar Engineering Conference*, Vol. **1**: 264-271.

Sherman, M., Sablok, A., Kopsov, and Chen, L. (2019). “Design of a Floating Spar Wind Platform with an Integrated Substructure and Tower.” *Offshore Technology Conference, Houston,* OTC-29375-MS.

Amaral, G. A., Pesce, C. P. and Franzini, G. R. (2022). "Mooring system stiffness: A six-degree-of-freedom closed-form analytical formulation." *Marine Structures,* **84**.

Kim, B. W., Sung, H. G., Kim, J. H. and Hong, S. Y. (2013). "Comparison of linear spring and nonlinear FEM methods in dynamic coupled analysis of floating structure and mooring system." *Journal of Fluids and Structures,* **42**, 205-227.

Dvorkin, E. N., Onate, E. and Oliver, J. (1988). "On a Non-Linear Formulation for Curved Timoshenko Beam Elements Considering Large Displacement Rotation Increments." *International Journal for Numerical Methods in Engineering,* **26**(7), 1597-1613.

Triantafyllou, M. S. and Hover, F. S. (2003). “MANEUVERING AND CONTROL OF MARINE VEHICLES”, *MIT Course 2.154 Class Notes.*

Lee, C.-H. (1995). “WAMIT Theory Manual”, *Massachusetts Institute of Technology.*

OCIMF (2020). “Static Towing Assembly Guidelines (STAG), First edition”, *Oil Companies International Marine Forum.*